



OPEN ACCESS

EDITED BY

Jonathan H. Tobias,
University of Bristol, United Kingdom

REVIEWED BY

Georgios S. Limouris,
National and Kapodistrian University of
Athens, Greece
Juan M. Colazo,
Vanderbilt University, United States

*CORRESPONDENCE

Jie Zhao
✉ zj666829@163.com

RECEIVED 22 December 2023

ACCEPTED 31 October 2024

PUBLISHED 20 November 2024

CITATION

Zhao G, Guan L, Zhang Y, Shi X, Luo W,
Yang M, Wang Q, Liu Z, Liu Y, Ding X and
Zhao J (2024) 18F-AIF-NOTA-octreotide PET/
CT and 3D printing technology for precision
diagnosis and treatment of phosphaturic
mesenchymal tumors in patients with tumor-
induced osteomalacia: two case reports.
Front. Endocrinol. 15:1359975.
doi: 10.3389/fendo.2024.1359975

COPYRIGHT

© 2024 Zhao, Guan, Zhang, Shi, Luo, Yang,
Wang, Liu, Liu, Ding and Zhao. This is an open-
access article distributed under the terms of
the [Creative Commons Attribution License
\(CC BY\)](https://creativecommons.org/licenses/by/4.0/). The use, distribution or reproduction
in other forums is permitted, provided the
original author(s) and the copyright owner(s)
are credited and that the original publication
in this journal is cited, in accordance with
accepted academic practice. No use,
distribution or reproduction is permitted
which does not comply with these terms.

18F-AIF-NOTA-octreotide PET/ CT and 3D printing technology for precision diagnosis and treatment of phosphaturic mesenchymal tumors in patients with tumor-induced osteomalacia: two case reports

Gang Zhao¹, Lijuan Guan², Yongqiang Zhang¹, Xingzhen Shi¹,
Wenming Luo¹, Maiqing Yang³, Qi Wang¹, Zhen Liu¹,
Yongqiang Liu¹, Xiaolei Ding⁴ and Jie Zhao^{1*}

¹Department of Orthopedics and Trauma, Weifang People's Hospital, First Affiliated Hospital of Shandong Second Medical University, Weifang, China, ²Nursing Department, Weifang Stomatology Hospital, Weifang, China, ³Department of Pathology, Weifang People's Hospital, First Affiliated Hospital of Shandong Second Medical University, Weifang, China, ⁴College of Traditional Chinese Medicine, Changchun University of Chinese Medicine, Changchun, Jilin, China

Objective: This study aims to report the application of 18F-AIF-NOTA-Octreotide PET/CT and 3D printing technology in the diagnosis and treatment of phosphaturic mesenchymal tumors (PMT) in patients with tumor-induced osteomalacia (TIO).

Case presentation: A 68-year-old male patient (Case 1) was admitted to the Weifang People's Hospital in August 2022 with complaints of "persistent pain in the bilateral flank and lumbosacral region". 18F-AIF-NOTA-Octreotide PET/CT showed high octreotide expression in the left femoral region. A 48-year-old male patient (Case 2) was admitted to the Weifang People's Hospital in November 2022, complaining of "pain in the lumbar region and ribs". 18F-AIF-NOTA-Octreotide PET/CT showed high octreotide expression in the pancreatic uncinate process and the left acetabulum. They were diagnosed with hypophosphatemic osteomalacia, with a strong consideration of an underlying neuroendocrine tumor. Preoperative design of 3D virtual surgery, CAD/CAM, and 3D printing technology were used to customize the digital surgical guide plates,

and the surgery was carried out. They were both finally confirmed as phosphaturic mesenchymal tumors (PMT) based on postoperative pathology and immunohistochemistry results. Both patients experienced substantial relief from their clinical manifestations after surgery.

Conclusion: 18F-AIF-NOTA-Octreotide PET/CT may be a precise diagnostic method for TIO, while 3D printing technology may serve as an effective and dependable adjunct for the treatment of PMT in patients with TIO.

KEYWORDS

phosphaturic mesenchymal tumors, tumor-induced osteomalacia, 18F-AIF-NOTA-octreotide PET/CT imaging, 3D printing technology, case reports

Introduction

Tumor-induced osteomalacia (TIO) is a rare paraneoplastic syndrome resulting from tumor-induced renal phosphate depletion and decreased bone mineralization, eventually leading to a series of adverse manifestations, including progressive skeletal pain, mobility impairments, and skeletal deformities (1, 2). TIO primarily arises due to the uncontrolled secretion of fibroblast growth factor-23 (FGF-23) by phosphaturic mesenchymal tumors (PMT) (3), preventing renal phosphate reabsorption and reducing intestinal phosphate absorption, leading to osteomalacia and the other signs and symptoms of TIO (4). The effective treatment of TIO requires thorough removal of the causative tumor using radiofrequency ablation (5, 6), and accurate localization of the tumor site is essential for successful outcomes, but it can be challenging. Previous studies have indicated that 18F-AIF-NOTA-Octreotide PET/CT can be used for the localization of neuroendocrine neoplasms (7, 8), but there is limited reporting on its application in the diagnosis and localization of TIO. 3D printing technology has been widely applied in orthopedics (9–13), but its application in TIO is also very limited. Herein, this study aims to report the application of 18F-AIF-NOTA-Octreotide PET/CT and 3D printing technology in the diagnosis and treatment of phosphaturic mesenchymal tumors (PMT) in patients with TIO.

Case presentation

Case 1

A 68-year-old male patient was admitted to the Weifang People's Hospital in August 2022, complaining of "persistent pain in the bilateral flank and lumbosacral region".

The physical examination showed increased pain in the neck and shoulder area during forward flexion, extension, and neck rotation. Spurling's test was positive, and there was tenderness

over the spinous processes of the posterior neck, as well as tenderness when pressing on the inner angles of both scapulae and the trapezius muscle in the neck and shoulder area. Tenderness was evident in the thoracic spine paravertebrally and over the chest. The straight leg raise test was positive at 70° on the right side, and Patrick's test (FABER test) was positive on the right side. The patient underwent surgical treatment for a right hip femoral neck fracture. Laboratory tests showed blood phosphorus levels of 0.53 mmol/L (normal range: 1.1–1.3 mmol/L), 25-hydroxy-VITD was 27.83 ng/ml (normal range: 8–30.5 ng/mL), and alkaline phosphatase (ALP) was 183 U/L (normal range: 40–150 U/L). 18F-AIF-NOTA-Octreotide PET/CT showed high octreotide expression in the left femoral region (Figure 1A). The patient was considered hypophosphatidic osteochondrosis, with a strong consideration of an underlying neuroendocrine tumor.

According to preoperative 18F-AIF-NOTA-Octreotide PET/CT imaging, preoperative design of 3D virtual surgery, CAD/CAM, and 3D printing technology were used to customize the digital surgical guide plates (Figure 1B). Following general anesthesia, the patient was placed in a prone position, and a Kocher-Langenbeck approach was used. The procedure involved sequential incisions through the skin, subcutaneous tissue, and deep fascia to expose the femur. A 3D-printed guide plate was then placed to determine the extent of the lesion. After examination, the guide plate showed good alignment, and Kirschner wires were drilled along the guide plate as per the direction and depth to determine the scope and cross-section of the lesion. The surface of the lesion showed a thin bone. Under the guidance of the guide plate, the grinding drill was used to remove the surface cortical bone of the lesion, exposing the localized lesion area. Soft tissue-like structures were observed within the bone, and the tumor was approximately 2 cm in size, with a grayish-red color. It had a relatively firm outer shell, while the tumor body itself was soft and elastic, with no adhesion. After complete excision and debridement of the sclerotic bone, allograft bone particles from freeze-dried cancellous bone were placed in the bone defect area, followed by layer-by-layer suturing. Blood loss was 100 mL, and the surgical time was 1 h.

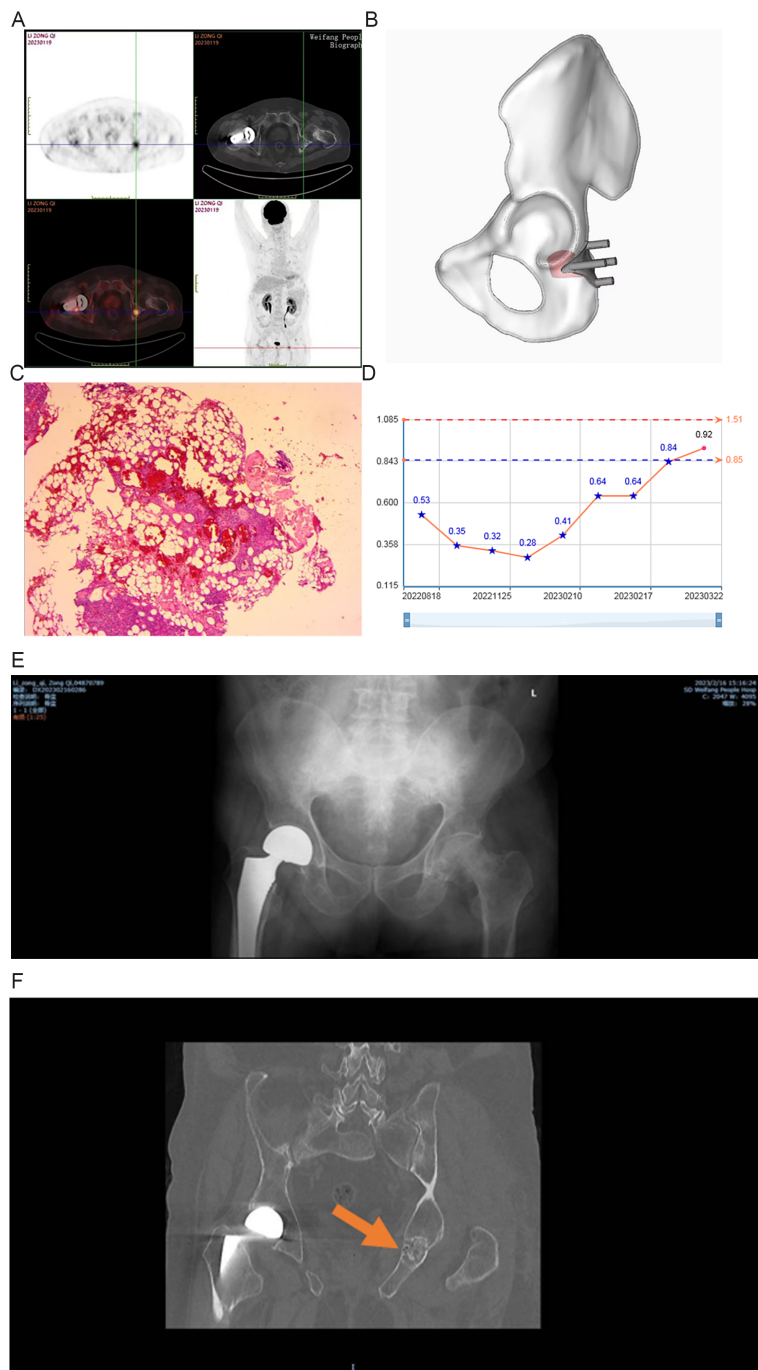


FIGURE 1
 Case 1: (A) a: 18F-ALF-NOTA-Octreotide PET/CT imaging results; (B) 3D-printed guide plate; (C) Hematoxylin & eosin staining; (D) Blood phosphorus changes; (E) X-ray after surgery; (F) CT during reexamination.

The postoperative pathology showed spindle-shaped cell proliferation in the bone marrow tissue, accompanied by vascular and adipose tissue proliferation, resembling a structure similar to vascular smooth muscle lipoma. Localized chondroid calcification was also observed. Immunohistochemistry showed Vimentin (+), CD56 (+), BCL-2 (+), SATB-2 (+), CD99 (+), stat6 (cytoplasmic +), SSTR-2 (+), CD34 (vascular +), CD68 (little +), Ki-67 (3%). The patient was finally confirmed as PMT according to pathology results (Figure 1C).

Two months after the surgery, the patient experienced significant relief in pain in the lumbosacral and hip regions, the VAS (Visual Analog Scale) score became 0 points, and the blood phosphorus levels increased to 0.92 mmol/L. The patient was administrated with oral calcium carbonate with vitamin D3 granules until blood phosphorus levels returned to normal (Figure 1D). X-ray and CT after surgery indicated the local bone density was enriched after implantation (Figures 1E, F).

Case 2

A 48-year-old male patient was admitted to the Weifang People’s Hospital in November 2022, complaining of “pain in the lumbar region and ribs”. The physical examination showed tenderness and pain upon palpation of the thoracolumbar spinous processes, paravertebral region, and chest ribs, with discomfort during movement. Laboratory tests showed blood phosphorus at 0.46 mmol/L and the 25-hydroxy-VITD of 9.45 ng/ml. The 18F-AIF-NOTA-Octreotide PET/CT showed high octreotide expression in the pancreatic uncinate process and the

left acetabulum. The patient was diagnosed with hypophosphatemic osteomalacia, with a strong consideration of an underlying neuroendocrine tumor (Figure 2A).

After general anesthesia, the procedure involved the use of an ilioinguinal approach, partial periosteal dissection to expose the internal plate of the ilium, and placement of a 3D-printed guide plate (Figures 2B, C). The examination showed that the guide plate matched the acetabulum well. Kirschner wires were drilled around the guide plate as per the preoperative design, and Kirschner wires were inserted to delineate the lesion area. Under the guidance of the guide plate, a micro saw was used to make an incision at

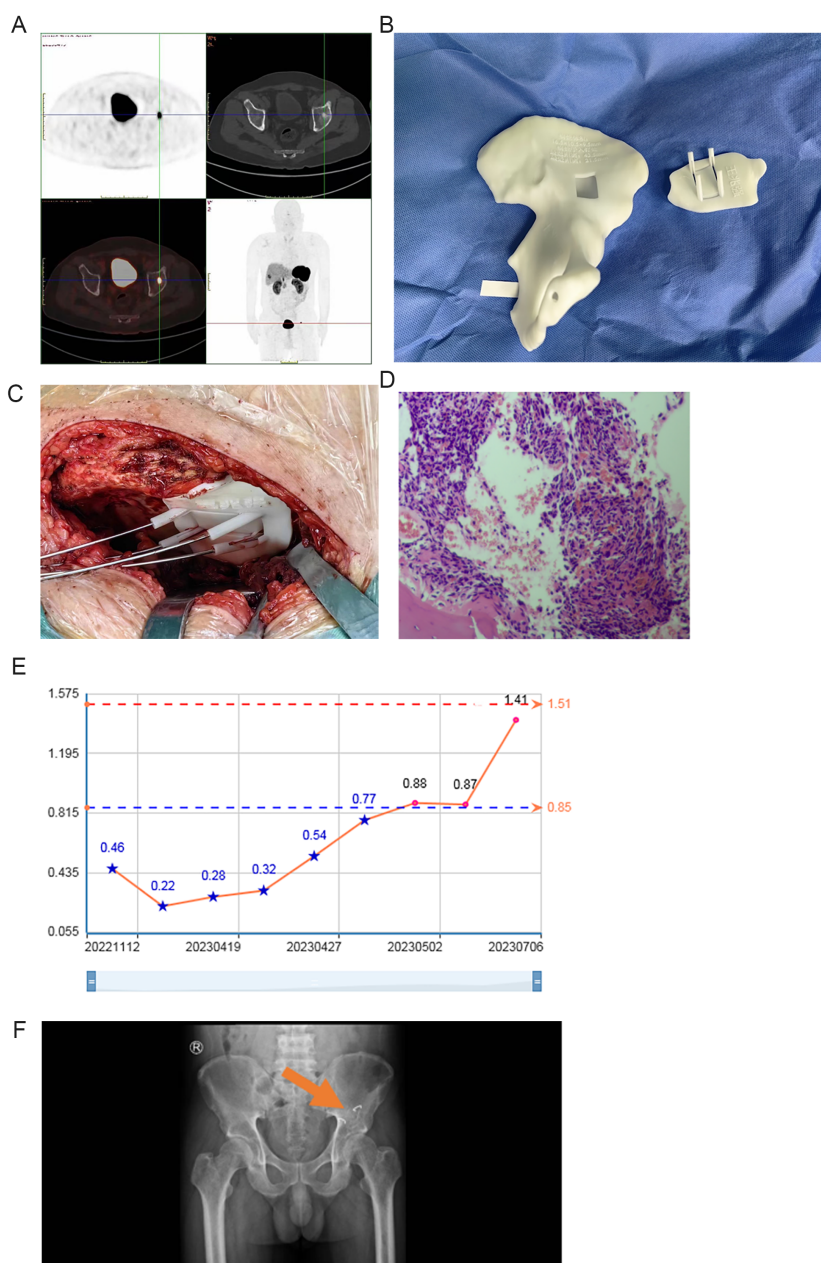


FIGURE 2 Case 2: (A) 18F-AIF-NOTA-Octreotide PET/CT imaging results; (B) 3D-printed guide plate; (C) 3D-printed guide plate use during surgery; (D) Hematoxylin & eosin staining; (E) Blood phosphorus changes. (F) X-ray after surgery.

the appropriate angle and depth in the proximal cortical bone of the lesion, which was set aside, exposing the localized lesion area. The bone knife was used to remove the lesion's bone, which contained a small amount of soft tissue with unclear boundaries. The excision was extended beyond the preoperative targeted area until a portion of the femoral head was exposed. The deficient area was reconstructed using a bone graft from the iliac wing and compacted and rectangular bone pieces were placed, followed by fixation with arch-shaped nails. Blood loss was 200 mL, and the surgical time was 1.5 h.

The postoperative pathology results confirmed the presence of PMT (Figure 2D).

The patient's systemic bone pain disappeared, and he was able to walk independently after postoperative 4 months. Blood phosphorus was 1.41 mmol/L, and the 25-hydroxy-VITD was 32.88 ng/ml in July 2023. Oral calcium carbonate D3 granules were administered postoperatively until the blood phosphorus returned to normal (Figure 2E). The postoperative X-ray shows an increase in local bone density after implantation (Figure 2F).

Discussion

This study presents two cases of TIO due to PMT, who were examined through 18F-AlF-NOTA-Octreotide PET/CT and treated with the assistance of 3D digital surgical guide plates, which may offer valuable insights for the diagnosis and management of PMT in patients with TIO. The two patients underwent 18F-AlF-NOTA-Octreotide PET/CT because it was more accessible than 68Ga-DOTATATE PET/CT at the primary hospital where the patients were admitted. In addition, a previous study indicated that 18F-AlF-NOTA-Octreotide could achieve at least comparable performance to 68Ga-DOTATATE/NOC (14).

The diagnosis of TIO can be challenging. Computer tomography (CT), magnetic resonance imaging (MRI), and other imaging techniques might not consistently identify TIO or precisely locate lesions in unique or uncommon anatomical regions (15). In the two cases, the implementation of 18F-AlF-NOTA-Octreotide PET/CT facilitated the precise diagnosis of TIO.

3D printing technology, as a concentrated embodiment of digital technology, is an effective means to realize the individualization and precision of various orthopedic surgeries. According to a previous study exploring the role of 3D printed surgical guides in the resection and reconstruction of malignant bone tumors, the blood loss, resection length, and complication rates were significantly lower in the 3D printed surgical guide group than in the control group (16). A recent study indicated that the use of 3D-printed guides could be used to create patient-specific bone grafts to manage glenoid deformity (17). Such guides can also be used for precise bone lesion resection (18–23), allowing the precise removal of the tumors while minimally compromising the bone structure. Still, no previous study examined the use of such guides in patients with TIO. In this study, the 3D guide plate could accurately guide the direction and depth of the channel of screws and determine the cross-section, the distance, and the relationship

between each other into the angle, etc., thus resulting in increased surgical accuracy and safety, shortened operating time, reduced intraoperative bleeding and side injuries. Furthermore, the application of 3D printing facilitates some parts of the operation that are more complicated and difficult in traditional surgeries. As a result, the use of 3D-printed guiding plate result in shorter surgeries and smaller blood losses (24, 25).

A limitation of the two cases reported here is that FGF23 was not measured; it is not a routine test at the authors' hospital. Only two cases were reported here, preventing comparison with controls and the evaluation of the patient outcomes.

Conclusion

This study indicated that 18F-AlF-NOTA-Octreotide PET/CT may be a precise diagnostic method for TIO, while 3D printing technology may serve as an effective and dependable adjunct for the treatment of TIO deprived from PMT, which provided a valuable reference for the diagnosis and treatment of TIO.

Data availability statement

The original contributions presented in the study are included in the article/supplementary material. Further inquiries can be directed to the corresponding author.

Ethics statement

The studies involving humans were approved by the Weifang City People's Hospital medical research Ethics Committee (KYL20231019-1). All patients provided written informed consent prior to treatment. The studies were conducted in accordance with the local legislation and institutional requirements. The participants provided their written informed consent to participate in this study. Written informed consent was obtained from the participant/patient(s) for the publication of this case report.

Author contributions

GZ: Writing – review & editing, Writing – original draft, Resources, Project administration, Methodology, Conceptualization. LG: Writing – review & editing, Writing – original draft, Validation, Resources, Methodology, Investigation. YZ: Writing – review & editing, Writing – original draft, Visualization, Methodology, Investigation, Formal analysis. XS: Writing – review & editing, Writing – original draft, Visualization, Supervision, Software, Project administration. WL: Writing – review & editing, Writing – original draft, Visualization, Validation, Software, Methodology. MY: Writing – review & editing, Writing – original draft, Visualization, Supervision, Software, Project administration. QW: Writing – review & editing, Writing – original draft, Visualization, Supervision,

Software, Project administration, Investigation. ZL: Writing – review & editing, Writing – original draft, Software, Resources, Methodology, Formal analysis. YL: Writing – review & editing, Writing – original draft, Validation, Software, Resources, Data curation. XD: Writing – review & editing, Writing – original draft, Validation, Supervision, Resources, Conceptualization. JZ: Writing – review & editing, Writing – original draft, Visualization, Supervision, Project administration, Investigation.

Funding

The author(s) declare that no financial support was received for the research, authorship, and/or publication of this article.

References

- Crotti C, Zucchi F, Alfieri C, Caporali R, Varenna M. Long-term use of burosumab for the treatment of tumor-induced osteomalacia. *Osteoporos Int.* (2023) 34:201–6. doi: 10.1007/s00198-022-06516-6
- Dahir K, Zanchetta MB, Stanciu I, Robinson C, Lee JY, Dhaliwal R, et al. Diagnosis and management of tumor-induced osteomalacia: perspectives from clinical experience. *J Endocr Soc.* (2021) 5:bvab099. doi: 10.1210/jendso/bvab099
- Jan de Beur SM, Miller PD, Weber TJ, Peacock M, Insogna K, Kumar R, et al. Burosumab for the treatment of tumor-induced osteomalacia. *J Bone Miner Res.* (2021) 36:627–35. doi: 10.1002/jbmr.4233
- Courbebaiss M, Lanske B. Biology of fibroblast growth factor 23: from physiology to pathology. *Cold Spring Harb Perspect Med.* (2018) 8. doi: 10.1101/cshperspect.a031260
- Tella SH, Amalou H, Wood BJ, Chang R, Chen CC, Robinson C, et al. Multimodality image-guided cryoablation for inoperable tumor-induced osteomalacia. *J Bone Miner Res.* (2017) 32:2248–56. doi: 10.1002/jbmr.3219
- Haffner D, Leifheit-Nestler M, Grund A, Schnabel D. Rickets guidance: part II-management. *Pediatr Nephrol.* (2022) 37:2289–302. doi: 10.1007/s00467-022-05505-5
- Long T, Yang N, Zhou M, Chen D, Li Y, Li J, et al. Clinical application of 18F-AIF-NOTA-Octreotide PET/CT in combination with 18F-FDG PET/CT for imaging neuroendocrine neoplasms. *Clin Nucl Med.* (2019) 44:452–8. doi: 10.1097/rlu.0000000000002578
- Long T, Hou J, Yang N, Zhou M, Li Y, Li J, et al. Utility of 18F-AIF-NOTA-Octreotide PET/CT in the localization of tumor-induced osteomalacia. *J Clin Endocrinol Metab.* (2021) 106:e4202–9. doi: 10.1210/clinem/dgab258
- Albergo JI, Farfalli GL, Ayerza MA, Ritacco LE, Aponte-Tinao LA. Computer-assisted surgery (CAS) in orthopedic oncology. Which were the indications, problems and results in our first consecutive 203 patients? *Eur J Surg Oncol.* (2021) 47:424–8. doi: 10.1016/j.ejso.2020.06.008
- Farfalli GL, Albergo JI, Piuze NS, Ayerza MA, Muscolo DL, Ritacco LE, et al. Is navigation-guided en bloc resection advantageous compared with intralesional curettage for locally aggressive bone tumors? *Clin Orthop Relat Res.* (2018) 476:511–7. doi: 10.1007/s11999.0000000000000054
- Farfalli GL, Albergo JI, Ritacco LE, Ayerza MA, Milano FE, Aponte-Tinao LA. What is the expected learning curve in computer-assisted navigation for bone tumor resection? *Clin Orthop Relat Res.* (2017) 475:668–75. doi: 10.1007/s11999-016-4761-z
- Laitinen MK, Parry MC, Albergo JI, Grimer RJ, Jeys LM. Is computer navigation when used in the surgery of iliosacral pelvic bone tumours safer for the patient? *Bone Joint J.* (2017) 99-B:261–6. doi: 10.1302/0301-620X.99B2.BJJ-2016-0149.R2
- Ritacco LE, Milano FE, Farfalli GL, Ayerza MA, Muscolo DL, Albergo JI, et al. Virtual planning and allograft preparation guided by navigation for reconstructive oncologic surgery: A technical report. *JBJS Essent Surg Tech.* (2017) 7:e30. doi: 10.2106/JBJS.ST.17.00001

Conflict of interest

The authors declare that the research was conducted in the absence of any commercial or financial relationships that could be construed as a potential conflict of interest.

Publisher's note

All claims expressed in this article are solely those of the authors and do not necessarily represent those of their affiliated organizations, or those of the publisher, the editors and the reviewers. Any product that may be evaluated in this article, or claim that may be made by its manufacturer, is not guaranteed or endorsed by the publisher.

- Pauwels E, Cleeren F, Tshibangu T, Koole M, Serdons K, Boeckxstaens L, et al. (18)F-AIF-NOTA-Octreotide outperforms (68)Ga-DOTATATE/NOC PET in neuroendocrine tumor patients: results from a prospective, multicenter study. *J Nucl Med.* (2023) 64:632–8. doi: 10.2967/jnumed.122.264563
- Bosman A, Palermo A, Vanderhulst J, De Beur SMJ, Fukumoto S, Minisola S, et al. Tumor-induced osteomalacia: A systematic clinical review of 895 cases. *Calcif Tissue Int.* (2022) 111:367–79. doi: 10.1007/s00223-022-01005-8
- Wang F, Zhu J, Peng X, Su J. The application of 3D printed surgical guides in resection and reconstruction of Malignant bone tumor. *Oncol Lett.* (2017) 14:4581–4. doi: 10.3892/ol.2017.6749
- Karpyshyn JN, Bois AJ, Logan H, Harding GT, Bouliane MJ. 3D printed patient-specific cutting guides for bone grafting in reverse shoulder arthroplasty: A novel technique. *J Shoulder Elb Arthroplast.* (2023) 7:24715492231162285. doi: 10.1177/24715492231162285
- Biscaccianti V, Fragnaud H, Hascoet JY, Crenn V, Vidal L. Digital chain for pelvic tumor resection with 3D-printed surgical cutting guides. *Front Bioeng Biotechnol.* (2022) 10:991676. doi: 10.3389/fbioe.2022.991676
- Li Z, Lu M, Min L, Luo Y, Tu C. Treatment of pelvic giant cell tumor by wide resection with patient-specific bone-cutting guide and reconstruction with 3D-printed personalized implant. *J Orthop Surg Res.* (2023) 18:648. doi: 10.1186/s13018-023-04142-4
- Gernandt S, Tomasella O, Scolozzi P, Fenelon M. Contribution of 3D printing for the surgical management of jaws cysts and benign tumors: A systematic review of the literature. *J Stomatol Oral Maxillofac Surg.* (2023) 124:101433. doi: 10.1016/j.jormas.2023.101433
- Gharbi MA, Zendeoui A, Tborbi A, Bouzidi R, Ezzaouia K, Nefiss M. Conservative surgical management of surface osteosarcoma using 3D printing technology: An unusual case report and literature review. *Int J Surg Case Rep.* (2023) 113:109086. doi: 10.1016/j.ijscr.2023.109086
- Gasparro MA, Gusho CA, Obioha OA, Colman MW, Gitelis S, Blank AT. 3D-printed cutting guides for resection of long bone sarcoma and intercalary allograft reconstruction. *Orthopedics.* (2022) 45:e35–41. doi: 10.3928/01477447-20211124-07
- Park JW, Kang HG, Kim JH, Kim HS. The application of 3D-printing technology in pelvic bone tumor surgery. *J Orthop Sci.* (2021) 26:276–83. doi: 10.1016/j.jos.2020.03.004
- Gigi R, Gortzak Y, Barriga Moreno J, Golden E, Gabay R, Rumack N, et al. 3D-printed cutting guides for lower limb deformity correction in the young population. *J Pediatr Orthop.* (2022) 42:e427–34. doi: 10.1097/BPO.0000000000002104
- Oraa J, Beitia M, Fiz N, Gonzalez S, Sanchez X, Delgado D, et al. Custom 3D-printed cutting guides for femoral osteotomy in rotational malalignment due to diaphyseal fractures: surgical technique and case series. *J Clin Med.* (2021) 10. doi: 10.3390/jcm10153366